RESEARCH ARTICLE SUMMARY

TRANSCRIPTION

Steps toward translocation-independent RNA polymerase inactivation by terminator ATPase ρ

Nelly Said*, Tarek Hilal*, Nicholas D. Sunday, Ajay Khatri, Jörg Bürger, Thorsten Mielke, Georgiy A. Belogurov, Bernhard Loll, Ranjan Sen, Irina Artsimovitch†, Markus C. Wahl†

INTRODUCTION: Factor-dependent transcription termination is essential to limit pervasive transcription, maintain genome stability, balance the expression of neighboring genes, and recycle RNA polymerase (RNAP). Two main classes of models can explain how termination factors stop RNA synthesis. In RNA-centric models, a terminator, powered by adenosine triphosphate (ATP)–dependent RNA translocase activity or by exonucleolytic RNA degradation, moves along the nascent RNA and rear-ends RNAP, dislodging it from the RNA. In transcription elongation complex (EC)–centric models, a terminator induces conformational changes in RNAP that inactivate it. Evidence in support of both mechanisms exists for translocases and exonucleases that elicit termination in bacteria and eukaryotes, but molecular details of their actions remain elusive because, once committed to termi-

nation, transcription complexes disassemble rapidly and are thus refractory to structure/function analyses.

RATIONALE: To elucidate the structural basis for termination, we used the archetypal ring-shaped hexameric helicase ρ. *Escherichia coli* ρ, perhaps the strongest molecular motor known, can load onto free RNA as an open ring, close the ring around the RNA, and engage in ATP-dependent translocation, removing any obstacle from its path. During transcription, ρ triggers RNA release from the EC within a well-defined termination zone once ~90 nucleotides of C-rich RNA, which ρ binds with high affinity, have been synthesized by RNAP. We surmised that a ρ-bound EC poised to enter this termination zone will be metastable, giving rise to an ensemble of intermediates en route to termination. We used single-particle cryo–

electron microscopy (cryo-EM) to analyze these "peri-termination" *E. coli* ECs bound to ρ, an ATP analog, and general elongation factors NusA and NusG known to modulate ρ activity. We also carried out in vitro and in vivo functional assays to validate key interactions suggested by our structural analysis.

RESULTS: We report the structures of seven intermediates along the termination pathway. ρ is recruited to the EC via extensive contacts to RNAP, NusA, and NusG, but initially makes no contacts with RNA. After recruitment, rearrangements of the ρ hexamer, NusA, upstream DNA, and several regions of RNAP set up a stage for RNA engagement by ρ. The N-terminal zinc-binding domain of the RNAP β′ subunit aids ρ in capturing the nascent RNA, a synergy that is supported by in vivo analysis of ρ and β′ mutants. Upon anchoring the RNA, ρ induces structural rearrangements that lead to the displacement of NusG and weakening of the RNAP grip on nucleic acids due to partial opening of the β′ clamp domain. The formation of a moribund complex, in which the clamp is wide open and the RNA is dislodged from the active site, completes the RNAP inactivation by ρ. Remarkably, the ρ ring is held open by the network of ρ contacts with RNAP and NusA throughout the entire pathway, preventing ρ from exerting force on RNA. Our data argue that ρ travels with RNAP rather than chases after it, and that termination is favored by pause-promoting conformational changes in the EC rather than by the reduced rate of RNA synthesis.

CONCLUSION: This study explains how ρ is targeted to RNAs that are still being made and cooperates with NusA and NusG to effect striking conformational changes that inactivate the transcribing RNAP. Hitchhiking on RNAP enables ρ to survey and silence useless and harmful transcripts independently of their sequence, as documented for several bacterial ρ orthologs. Unexpectedly, ρ stalls transcription without engaging its powerful motor activity, which may be essential after termination to destroy R-loops, the toxic by-products of the EC dissociation. A growing list of allosteric mechanisms of transcription regulation suggests that many accessory factors may exploit dynamic properties of RNAP to modulate RNA synthesis, acting together with the orthologs/analogs of Nus factors present in all domains of life. ∎
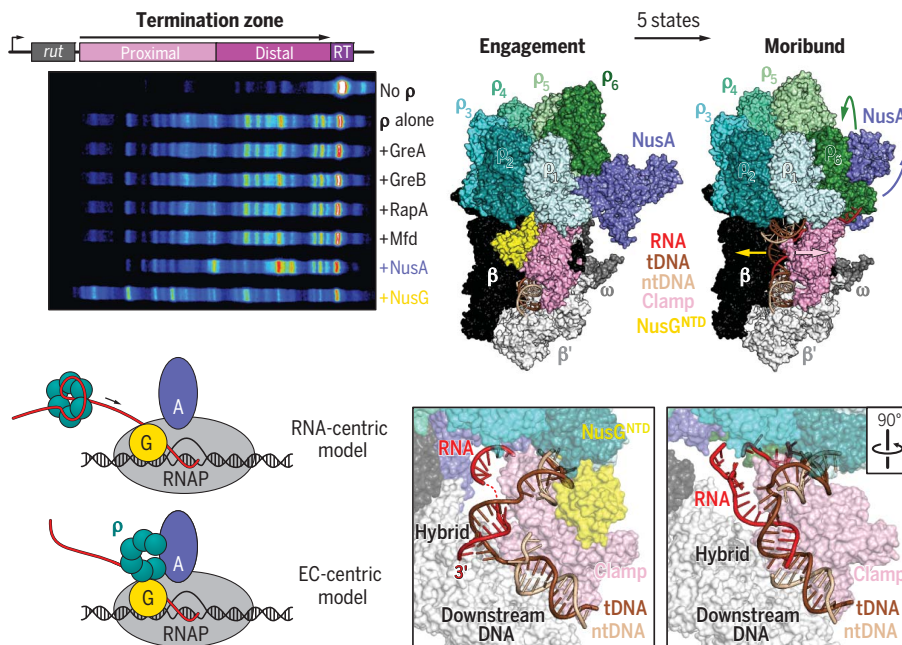
ρ traps NusA/NusG-modified elongation complexes in a moribund state. NusA and NusG are the only general transcription factors in *E. coli* that modulate ρ-dependent termination. Conflicting models explain how ρ terminates RNA synthesis. Cryo-EM analysis of ρ/NusA/NusG-ECs and structure-informed biochemical analyses support an EC-centric model, revealing how an initial engagement complex is converted stepwise to a moribund complex. The pathway involves rearrangements of ρ, NusA/G, and RNAP elements, and culminates in a massive displacement of the RNA 3′-end from the RNAP active site.

READ THE FULL ARTICLE AT
https://doi.org/10.1126/science.abd1673

TRANSCRIPTION

Steps toward translocation-independent RNA polymerase inactivation by terminator ATPase ρ

Nelly Said[1]*, Tarek Hilal[2]*, Nicholas D. Sunday[3], Ajay Khatri[4,5], Jörg Bürger[6,7], Thorsten Mielke[6], Georgiy A. Belogurov[8], Bernhard Loll[1], Ranjan Sen[4], Irina Artsimovitch[3]†, Markus C. Wahl[1,9]†

Factor-dependent transcription termination mechanisms are poorly understood. We determined a series of cryo–electron microscopy structures portraying the hexameric adenosine triphosphatase (ATPase) ρ on a pathway to terminating NusA/NusG-modified elongation complexes. An open ρ ring contacts NusA, NusG, and multiple regions of RNA polymerase, trapping and locally unwinding proximal upstream DNA. NusA wedges into the ρ ring, initially sequestering RNA. Upon deflection of distal upstream DNA over the RNA polymerase zinc-binding domain, NusA rotates underneath one capping ρ subunit, which subsequently captures RNA. After detachment of NusG and clamp opening, RNA polymerase loses its grip on the RNA:DNA hybrid and is inactivated. Our structural and functional analyses suggest that ρ, and other termination factors across life, may use analogous strategies to allosterically trap transcription complexes in a moribund state.

Pervasive transcription of cellular genomes is kept in check by surveillance mechanisms that ensure that the synthesis of unwanted RNAs is terminated early. In bacteria, this function is performed by ρ, originally identified as a factor that terminates transcription in *Escherichia coli* bacteriophage λ (*1*). *E. coli* ρ defines boundaries of many transcription units (*2*), silences horizontally acquired genes and antisense RNAs (*2–4*), removes stalled RNA polymerase (RNAP) from the path of the replisome to maintain chromosome integrity (*5*), and inhibits R-loop formation (*6*). Five decades of mechanistic studies of *E. coli* ρ led to a model in which its motor activity takes center stage. ρ is a hexameric ring-shaped RecA-family RNA translocase that exists in open and closed states capable of loading onto RNA and translocation, respectively (*7*). A ρ monomer is composed of two domains. The N-terminal domain (NTD) contains a primary RNA-binding site (PBS) that engages unstructured C-rich ρ-utilization (*rut*) sites;

the C-terminal domain (CTD) contains the secondary RNA-binding site (SBS) and ATPase/translocase determinants. After *rut* recognition, the ring closes, trapping RNA at the SBSs in a central pore (*7*). The closed hexamer engages in ATP-powered 5′-to-3′ translocation along the RNA toward RNAP, maintaining contacts to the *rut* RNA, a race described as "kinetic coupling" (*8*). When RNAP pauses, ρ catches up and dissociates an otherwise very stable elongation complex (EC) by a still-debated mechanism (*9*).

Primed by a canonical *rut* site, ρ terminates transcription by phage and eukaryotic RNAPs (*10*, *11*) and displaces streptavidin from a biotin anchor (*12*), which implies that ρ could dissociate any EC. However, in the context of the physiological mechanism, glaring discrepancies have been noted. For example, ρ[R353A] is severely defective in ring closure but terminates efficiently, whereas ρ[W381A] closes readily but has termination defects (*13*, *14*). A lack of perfect correlation among ATPase, helicase, and termination activities suggests that ρ motor and termination functions are separable and that ρ/RNAP interactions, first reported in 1984 (*15*), may control termination. Direct interactions with RNAP would also explain how ρ is targeted to actively synthesized RNAs and excluded from completed transcripts. Furthermore, the elongation factors NusA and NusG modulate termination. NusA stimulates ρ binding to RNAP (*15*), yet paradoxically delays termination in vitro (*16*). NusG promotes early termination (*17*); it allosterically stimulates ring closure (*13*, *18*), enabling ρ to act at noncanonical sites (*2*). In support of ρ trafficking with the EC in vivo, chromatin immunoprecipitation with DNA microarray (ChIP-chip) analysis showed that ρ and NusA bind to RNAP

immediately after promoter escape, with NusG lagging behind (*19*). An allosteric model, in which ρ is recruited to RNAP rather than RNA and traps the EC in an inactive state prior to dissociation (*20*), explains how ρ is excluded from transcripts that have been released from RNAP. However, although RNAP substitutions that confer resistance to ρ are known (*8*), they are unlikely to alter RNAP binding to ρ. Instead, these mutant RNAPs are insensitive to pauses and are thought to simply outrun ρ.

To reveal ρ action in the context of complete *E. coli* ρ/NusA/NusG/*rut* ECs (ρ-ECs), we elucidated their atomic structures by single-particle cryo–electron microscopy (cryo-EM) and conducted structure-guided functional analyses. Our data are consistent with a series of steps along a termination pathway, in which ρ allosterically inactivates the EC via interactions with RNAP, NusA, NusG, upstream DNA, and *rut* RNA.

NusA and NusG are the only general elongation factors that modulate ρ

Six general elongation factors are present in *E. coli*: NusA, NusG, cleavage factors GreA/B, recycling factor RapA, and transcription-repair coupling factor Mfd. We assessed their potential effects in vitro on a DNA template encoding bacteriophage λ tR1, an archetypical ρ-dependent terminator (figs. S1A and S2A). In the absence of other proteins, RNAP generated predominantly read-through (RT) transcripts. ρ alone promoted termination at several sites; NusG stimulated RNA release at promoter-proximal sites, whereas NusA shifted the termination window downstream (fig. S1). By contrast, the Gre factors, RapA, and Mfd did not alter the efficiency or pattern of ρ-dependent termination (fig. S1A). We conclude that a minimal system to study termination comprises EC, NusA, NusG, and ρ.

Assembly and structural analysis of ρ-ECs

Whereas ECs are readily amenable to structural studies, RNAP dissociates rapidly once committed to termination. We assembled ECs on a DNA scaffold with a 15–base pair (bp) downstream DNA (dDNA), a 9-nucleotide bubble, and a 30-bp upstream DNA (uDNA). The 99-nucleotide RNA contained the λ tR1 *rut* region (also used in all transcription assays; fig. S1A), which is followed by a well-defined ρ release window on long templates (fig. S2). However, in this scaffold RNAP is poised at the upstream edge of the ρ termination region so as to capture the metastable complex prior to dissociation. ρ-ECs were assembled stepwise with Nus factors, incubated with the ATP analog ADP-BeF₃ that supports ρ ring closure (*7*), and subjected to single-particle cryo-EM analysis without cross-linking (figs. S3 to S9). From ~10,000 micrographs, we chose ~2,100,000 particle images, ~390,000 of which represented ρ-ECs, whereas we discarded images of ECs lacking ρ,

[1]Laboratory of Structural Biochemistry, Institute of Chemistry and Biochemistry, Freie Universität Berlin, Berlin, Germany. [2]Research Center of Electron Microscopy and Core Facility BioSupraMol, Institute of Chemistry and Biochemistry, Freie Universität Berlin, Berlin, Germany. [3]Department of Microbiology and Center for RNA Biology, The Ohio State University, Columbus, OH, USA. [4]Laboratory of Transcription, Centre for DNA Fingerprinting and Diagnostics, Hyderabad, India. [5]Graduate Studies, Regional Centre for Biotechnology, Faridabad, Haryana, India. [6]Microscopy and Cryo-Electron Microscopy Service Group, Max-Planck-Institut für Molekulare Genetik, Berlin, Germany. [7]Institute of Medical Physics und Biophysics, Charité–Universitätsmedizin Berlin, Berlin, Germany. [8]Department of Biochemistry, University of Turku, FIN-20014 Turku, Finland. [9]Macromolecular Crystallography, Helmholtz-Zentrum Berlin für Materialien und Energie, Berlin, Germany.
*These authors contributed equally to this work.
†Corresponding author. Email: artsimovitch.1@osu.edu (I.A.); markus.wahl@fu-berlin.de (M.C.W.)
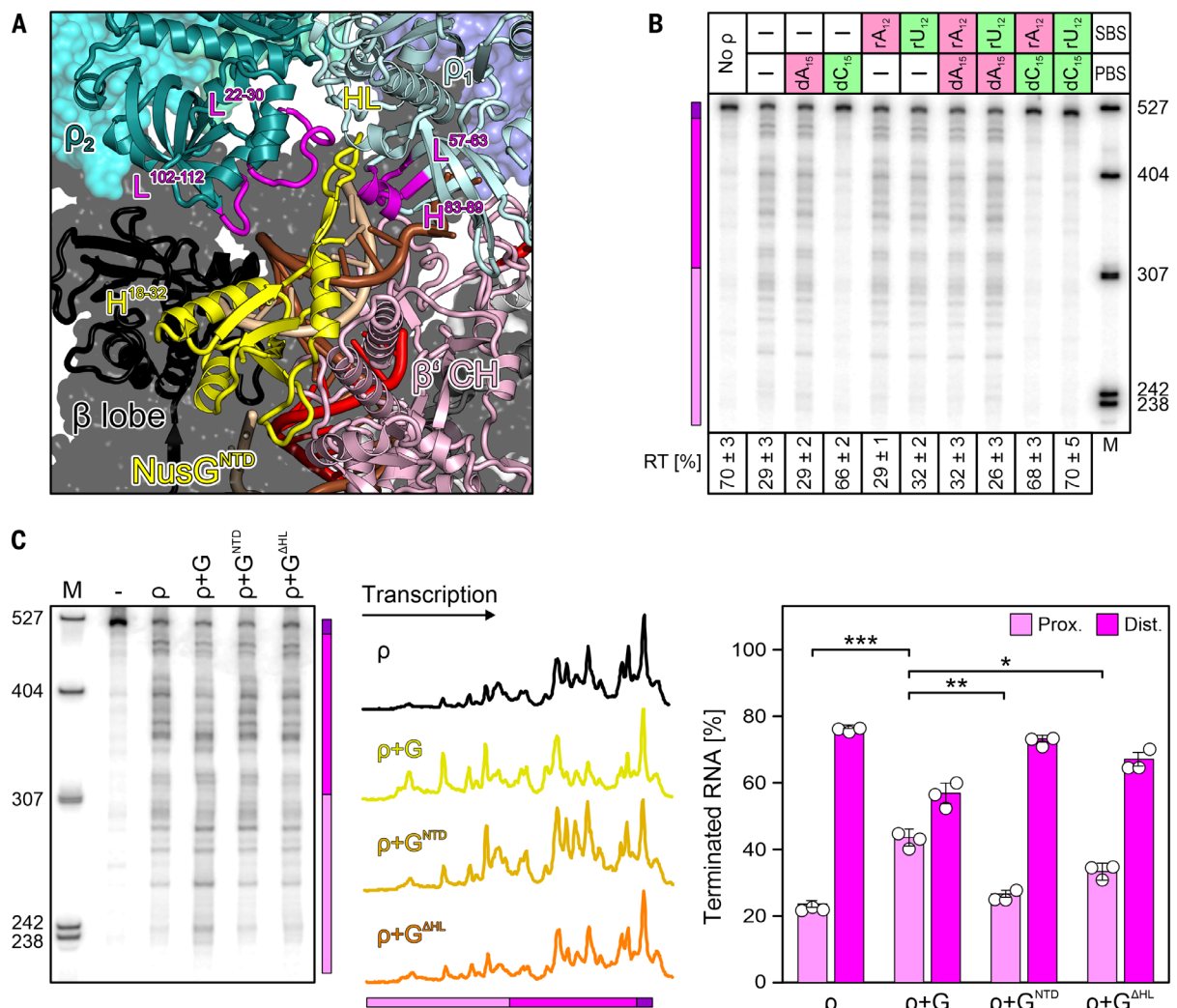
Fig. 1. Engagement. (**A**) Semitransparent surface/cartoon representations of the engagement complex, highlighting contact sites of ρ subunits. Rotation symbols in this and the following figures indicate views relative to the upper left panel of (A). (**B**) Post-translocated state of the nucleic acids at the active site. tDNA, template DNA; ntDNA, nontemplate DNA; +1, template nucleotide pairing with the next incoming NTP. (**C** to **H**) Close-up views of ρ/EC contacts. Elements in magenta are discussed in the text. (**I**) ρ-cutaway view; magenta denotes ρ-contacting RNAP elements around the RNA exit.

free RNAP, or free ρ. Multiparticle 3D refinement (21) led to nine cryo-EM maps corresponding to complexes I to V, I^ΔNusG, III^ΔNusG, IIIa, and IVa (fig. S4). The local resolution varied from below 3 Å in some core regions to 8 to 12 Å in some peripheral elements (figs. S5 to S7 and table S1). C-terminal regions of NusA were tentatively placed into weakly defined

cryo-EM density in the region where they reside in other ECs (22–24). Although backbones of all other described elements could be traced unequivocally, assignment of side-chain conformations is tentative at the present resolutions. Therefore, we used individual residues mostly as landmarks of specific regions.

Our cryo-EM structures can be sorted along a pathway in which ρ initially engages the EC, is then primed for *rut* RNA binding, subsequently captures *rut* RNA, and finally inactivates RNAP (fig. S1, B to J). In the following, we describe the main structures (complexes I to V) individually along this presumed sequence of events and then discuss how additional

Fig. 2. Effects of ρ PBS/SBS ligands and NusG^NTD. (**A**) Close-up view on NusG^NTD in the engagement complex. Elements discussed in the text are in magenta. (**B**) Effects of optimal (green) and poor (red) PBS/SBS ligands on ρ termination; here and in other figures, positions of proximal (pink) and distal (magenta) terminated RNAs and the read-through transcript (RT; purple) are indicated with a colored bar. PBS (dN₁₅) ligands were present at 5 μM, SBS (rN₁₂) ligands at 500 nM. The fraction of RT versus the sum of all RNA products is shown at the bottom. Values represent means ± SD of three independent experiments. (**C**) Modulation of ρ effects by the indicated NusG ("G") variants. Left: Transcription termination assays on the λ tR1 DNA template (see fig. S1A) analyzed on a 5% denaturing urea-acrylamide gel. Center: Lane profiles from the gel; the y-axis signals were normalized on the basis of total signal in that lane. Right: Distribution of ρ-terminated RNAs between the proximal and distal regions. Values represent means ± SD of three independent experiments. *P < 0.01, **P < 0.001, ***P < 0.0001 (unpaired Student t test).

structures fit into the picture. We encourage the reader to view animated versions of the process (movies S1 and S2) first.

EC engagement

The domain structures of NusA and NusG are shown in fig. S2C; table S2 lists relevant regions of RNAP and factors. In complex I (Fig. 1A, figs. S1B and S9, and movie S1), RNAP ($\alpha_2\beta\beta'\omega$ subunit composition) assumes a conformation observed in an unmodified post-translocated EC [25] [root mean square deviation (RMSD) of 1.24 Å for 2687 pairs of aligned Cα atoms; Fig. 1B]. NusG^NTD is bound at its canonical site [26] next to proximal uDNA (Fig. 2A). NusA^NTD is sandwiched between the β flap tip (FT) and α₁^CTD, as in a NusA-

modified hairpin-paused EC [22] (Fig. 1A). The NusA S1-KH RNA-binding region and AR1 extend outward across the β′ zinc-binding domain (β′ZBD), whereas AR2 angles down toward ω. Additional contacts of AR2 to α₂^CTD observed in [22] are possible and would explain how, in our structures, AR2 is displaced from an autoinhibitory position on NusA^S1-KH in isolated NusA [27], but are not clearly resolved in the map.

ρ adopts an open-ring conformation and binds above the active-site cleft around the β flap, with ρ^NTDs oriented toward RNAP (Fig. 1A). We tentatively modeled ADP-BeF₃ at the five intact nucleotide binding sites in this and other complexes. Looking from CTD to NTD, we labeled the protomers clockwise, ρ₁ to ρ₆,

starting at the ring opening (Fig. 1A), ρ₁^NTD lies next to β′ZBD, with β′ZBD-K39/R60 forming electrostatic contacts with ρ₁^E106 (Fig. 1C). One edge of ρ₁^CTD (Thr²⁷⁶) is positioned next to β^FT-P897 opposite NusA^NTD (Fig. 1D). Loop²⁰⁹⁻²¹³ and loop²³⁰⁻²³⁶ of ρ₁^CTD contact loop¹⁵³⁻¹⁵⁹ of NusA^S1 (Fig. 1D). The hairpin loop (HL) of NusG^NTD is bent over the proximal uDNA, sandwiched between loop⁵⁷⁻⁶³ and helix⁸³⁻⁸⁹ of ρ₁^NTD and loop²²⁻³⁰ of ρ₂^NTD (Fig. 2A). Loop¹⁰²⁻¹¹² of ρ₂^PBS lies on top of NusG^NTD helix¹⁸⁻³² while the ρ₂^PBS cavity hovers above the β lobe/protrusion (Fig. 2A). ρ₃^PBS accommodates helix¹⁰⁰⁴⁻¹⁰³⁷ of the lineage-specific β SI2 insertion while neighboring edges of the NTDs of ρ₃ (helix⁸³⁻⁸⁹) and ρ₄ (loop²¹⁻³¹) sandwich the globular tip of SI2 (Fig. 1E).
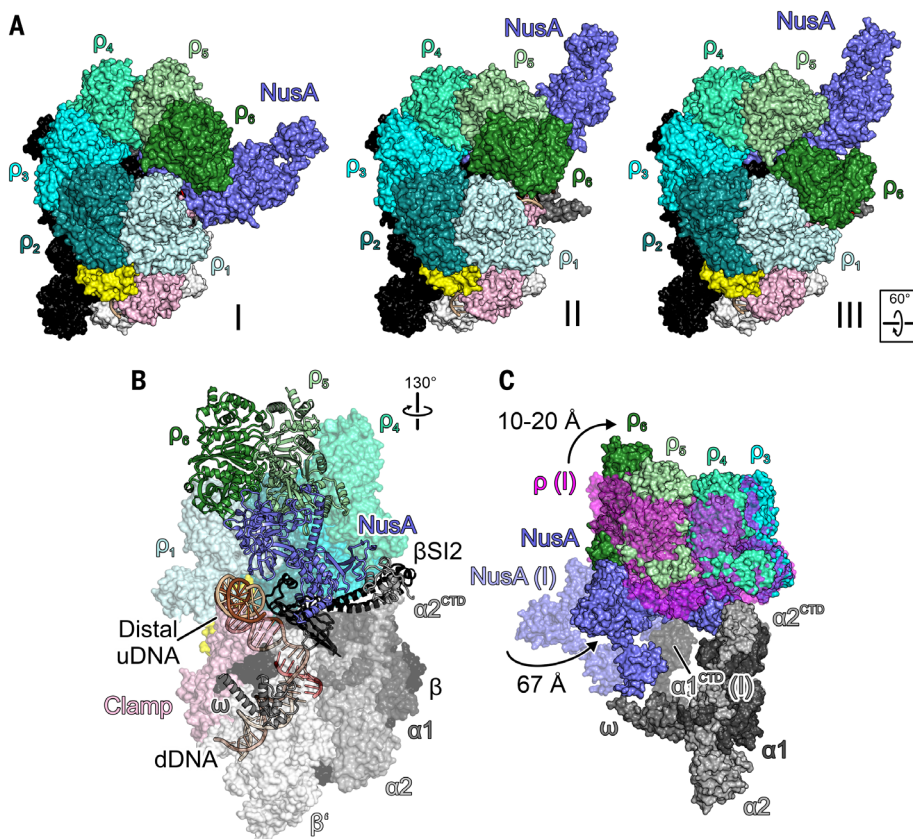
Fig. 3. Priming. (**A**) Surface views of the engagement (I), primed (II), and RNA capture (III) complexes, illustrating rotation of NusA underneath ρ_6 (I to II) and shift of ρ_6 from ρ_5 to ρ_1 (II to III). (**B**) Semitransparent surface/cartoon representations of the primed complex, highlighting contact sites of ρ subunits and distal uDNA on top of β'^{ZBD}. (**C**) Overlay of selected elements of the primed complex (solid surfaces) and engagement complex (semitransparent surfaces; ρ, magenta), highlighting movements of NusA and ρ as well as handover of NusA^{NTD} from α_1^{CTD} to α_2^{CTD}.

ρ_5^{PBS} binds the protruding loop$^{75-91}$ of NusA^{NTD}, and $\rho_5^{NTD-E106/E108}$ forms an electrostatic network with $\alpha_1^{CTD-K297/K298}$ (Fig. 1F). ρ_6 does not directly contact RNAP; instead, ρ_6^{PBS} rests on NusA^{S1-KH1}, opposite ρ_1^{CTD}, with direct ρ_6^{R88}-S1^{E136} and ρ_6^{K115}-KH1^{E219} contacts (Fig. 1G). Thus, ρ subunits engage multiple RNAP elements (FT, ZBD, lobe, SI2, α_1^{CTD}), NusG^{NTD}, and NusA$^{NTD-S1-KH1}$ (Fig. 1, C to H), which are circularly arranged around the RNA exit tunnel, matching the spiral pitch of—and thus stabilizing—the open ρ ring (Fig. 1I).

Multifaceted contacts with the EC may enable ρ to achieve a precisely tuned termination activity. For example, SI2 may be important for initial ρ recruitment, in which case its deletion should suppress termination, but SI2 blocks ρ_3^{PBS} (Fig. 1E) and helps to stabilize ρ in an open conformation, such that its deletion should promote termination. We found that SI2 deletion clearly shifted ρ termination to more promoter-proximal sites in vitro (fig. S10A). Interestingly, an opposite effect of ΔSI2 is observed in vivo (fig. S10B), supporting the idea of fine-tuning (e.g., by changes in the

chemical environment). NusA is also expected to exert opposing effects. Although observed ρ-NusA contacts and gel filtration data (fig. S2D) are in line with a reported contribution of NusA to ρ recruitment (15), NusA also hinders ρ ring closure: The S1 and KH1 domains are wedged between ρ_1 and ρ_6, with the β^{FT}/NusA^{NTD}/α_1^{CTD} array additionally stabilizing the ρ spiral (Fig. 1A). Furthermore, a clear but poorly contoured region of density above the RNA exit tunnel opening indicates flexible exiting RNA guided between NusA^{S1} and β'^{ZBD} (Fig. 1C). Thus, NusA keeps the ρ ring open and, acting with β'^{ZBD}, may sequester exiting RNA from ρ, as suggested previously (28). Both of these effects could explain how NusA delays ρ termination observed by us (fig. S1A) and others (16, 17).

A striking feature of complex I is continuous density, corresponding to single-stranded template DNA (tDNA) that extends from the proximal uDNA into ρ_1^{PBS} (Fig. 1H and Fig. 2A). The finding that ρ ATPase activity is stimulated by DNA ligands that can bind to PBS but not SBS (29) is commonly used to distinguish the

PBS and SBS effects, and DNA-PBS interactions were observed in structures (30) but were presumed to be artifactual. We used dN$_{15}$ and rN$_{12}$ oligomers specific for the PBS and SBS, respectively, to assess the importance of ρ-DNA interactions. Our results show that dC$_{15}$, the optimal PBS ligand (31), strongly inhibits termination (Fig. 2B) when present alone or with the SBS ligands. By contrast, dA$_{15}$, which does not bind PBS, or rU$_{12}$, a canonical SBS ligand (31), had no effect on ρ activity. These results support a model in which ρ^{PBS} interactions with tDNA are functionally important. However, it is also possible that dC$_{15}$ oligomers could compete with the nascent RNA at a later step in the pathway. Capture of uDNA would be expected to hinder continuous DNA movement through RNAP, revealing a first mechanism by which ρ can inhibit RNAP.

NusG^{HL} is pushed against and displaces the complementary nontemplate strand (Fig. 2A). To test whether HL contributes to termination, we replaced NusG residues 47 to 63 with two glycines and evaluated its effect in vitro. In the absence of NusG, ρ predominantly releases longer RNAs (distal region; Fig. 2C, magenta). Consistent with published reports (13, 17), wild-type NusG shifted the termination window upstream: The fraction of proximal ρ-terminated RNAs increased from 24 to 43% (Fig. 2C, violet). NusG^{ΔHL} was partially defective in stimulating early termination (33%), whereas the isolated NTD was almost completely inactive (27%), as shown previously (13, 32). On the basis of these findings, we interpret complex I as an engagement complex, from which ρ can trigger further steps toward termination.

Priming for RNA capture

In complex II, RNAP, NusG^{NTD}, the hybrid, dDNA, proximal uDNA, and ρ_1 to ρ_3 subunits are essentially unaltered. However, a drastic rotation of NusA^{NTD}/β^{FT} toward α^{NTD}s is observed (Fig. 3, A to C), and NusA^{NTD}-β^{FT} interactions change upon repositioning (Fig. 4A). The tip of NusA^{NTD} moves from ρ_5^{PBS} to ρ_4^{PBS}, with concomitant handover of NusA^{NTD} from α_1^{CTD} to α_2^{CTD}, which consolidates the NusA^{NTD}-ρ_4^{PBS} interaction (Fig. 3, B and C). NusA^{S1} now resides underneath ρ_6^{PBS} (Fig. 3B), and loop$^{213-221}$ of NusA^{KH1} is inserted between helix$^{83-89}$ of ρ_5 and loop$^{22-30}$ of ρ_6 (Fig. 4B). As NusA moves underneath, ρ_4, ρ_5, and ρ_6 are slanted upward (Fig. 3C).

While NusA has moved away from β'^{ZBD}, the distal uDNA duplex is running across the ZBD (Fig. 4C). Thus, the transition to complex II might be fueled by competition of distal uDNA and NusA for β'^{ZBD}, as well as by the interchangeability of the NusA^{NTD}/ρ_5/α_1^{CTD} (complex I) and NusA^{NTD}/ρ_4/α_2^{CTD} (complex II) interaction networks. Consistent with an earlier report (33), we found that deletion of α^{CTD}s modestly inhibited termination while essentially
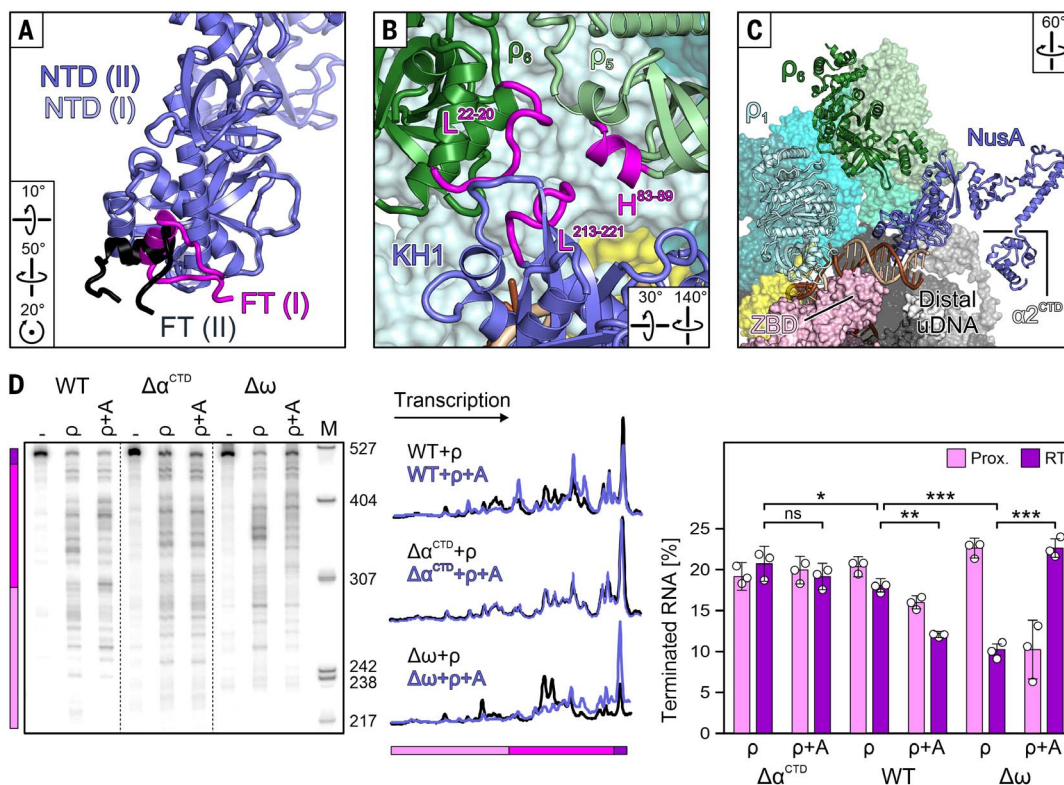
Fig. 4. NusA interactions. (**A**) Comparison of β^{FT}-NusA^{NTD} interactions in the primed and engagement complexes after superposition of NusA^{NTD}s. (**B**) ρ_5/ρ_6/NusA^{KH1} interaction network in the primed complex. (**C**) Correlation of accommodation of distal uDNA on the β'^{ZBD} and NusA rotation underneath ρ_6 in the primed complex. (**D**) NusA ("A") effects on termination by wild-type (WT) RNAP or by RNAP variants lacking α^{CTD}s or ω; dashed lines indicate spliced images. The RNA fractions are means ± SD of three independent experiments. *$P < 0.1$, **$P < 0.001$, ***$P < 0.0001$; ns, not significant.

eliminating the effect of NusA (Fig. 4D). In stark contrast, deletion of the ω subunit potentiated ρ termination and the NusA effect thereon (Fig. 4D). As NusA^{AR2} approaches ω in complex I (Fig. 1A) and as this interaction is broken in complex II, ω deletion may assist the transition to complex II.

ρ_6^{PBS} hovers ~45 Å above β'^{ZBD} and is not bound to RNA (Fig. 4C), but a weak neighboring density (not modeled) might indicate an approaching RNA. Thus, we consider complex II to be primed for RNA capture by ρ.

RNA capture

Upon transition to complex III, RNAP, dDNA, the hybrid, proximal uDNA, NusG^{NTD}, NusA, and ρ subunits 1 to 5 remain unaltered. In contrast, ρ_6 detaches from ρ_5, steps down by ~45 Å from on top of NusA^{KH1} in the primed complex to β'^{ZBD}, displacing distal uDNA, and links up with ρ_1 (Fig. 3A and Fig. 5A). ρ_6 now interacts laterally with NusA^{S1}, as does ρ_1 in the engagement complex (Fig. 5B). The ring opening thereby migrates from ρ_1/ρ_6 to ρ_6/ρ_5.

ρ_6^{PBS} captures two nucleotides of *rut* RNA and sandwiches them with the underlying β'^{ZBD}, while a rather featureless density next to β'^{ZBD} above the RNA exit represents exiting RNA (Fig. 5B). It can be envisaged that as ρ_6 steps down onto β'^{ZBD}, portions of RNA between

exiting RNA and the captured *rut* nucleotides are funneled into the open ρ ring (Fig. 5B). With the known pyrimidine preference of ρ^{PBS} (7, 30), we therefore tentatively assigned U24 and C25 from the upstream *rut* site (fig. S2B) as the ρ_6^{PBS} ligands. We term complex III the RNA capture complex, as ρ engages RNA for the first time.

The ZBD/RNA/ρ_6^{PBS} contacts observed in complex III suggest that ρ PBS variants could have synergistic defects with β'^{ZBD} variants. We screened for synthetic termination defects of β' variants in the presence of ρ^{Y80C}, which weakens *rut* affinity (34). We randomly mutagenized the *rpoC* gene on a plasmid and transformed the mutant library into *E. coli* ρ^{WT} or ρ^{Y80C} strains containing a chromosomal P_{RM}-*racR*-t_{rac}-*lacZYA* reporter fusion. t_{rac} is a NusG-dependent terminator at which ρ^{Y80C} exhibits a milder defect (35). Screening yielded a β'^{G82D} ZBD variant with a termination defect in combination with ρ^{Y80C} that was twice that observed with the wild type (Fig. 5C). A previously reported β'^{Y75N} substitution (36) had a similar effect (Fig. 5C). Many additional β'^{ZBD} variants constructed by site-directed mutagenesis—particularly C72H, C85H, and E86K—showed synthetic growth defects with ρ^{Y80C} (fig. S10C and table S3). The affected residues reside on the upper ZBD surface that

supports ρ_6^{PBS}-bound RNA (Fig. 5B), and substitutions of zinc-coordinating Cys^{72} and Cys^{85} likely disturb the ZBD structure. Although we cannot exclude the possibility that ZBD substitutions may affect other steps of RNA synthesis or its coupling to translation (37, 38), our results support the notion of direct ρ/ZBD cooperation revealed by the RNA capture complex.

EC inhibition

Several major changes distinguish complex IV from the RNA capture complex. The density for NusG^{NTD} is missing, and the bottom part of the uDNA duplex swings outward to a position where it would sterically clash with NusG^{NTD} (fig. S11A), while the template strand is partly pulled back from ρ_1^{PBS} (fig. S11B). The N-terminal part of the β' clamp rotates away from dDNA, widening the primary channel by ~8 Å (Fig. 6A), β^{lid} rearranges (fig. S11C), and β'^{SI3} and β^{jaw} pivot away from dDNA (fig. S11D). Concurrently with rearrangements in nucleic acid–guiding elements, the tDNA acceptor nucleotide is destabilized at the templating position (Fig. 6B), reminiscent of a paused bacterial EC (39) and an α-amanitin–stalled eukaryotic RNAPII (40).

ρ-induced rearrangements of the lid, SI3, or jaw suggest that their removal may influence

Fig. 5. RNA capture. (**A**) Surface view of the RNA capture complex (nucleic acids as cartoon) with superimposed ρ_6 from the primed complex. Arrow indicates movement of ρ_6 during the transition from the primed to the RNA capture state. (**B**) Close-up views of ρ_6^{PBS} with bound RNA. Arrows show the direction of intervening RNA region that might ascend 5′-to-3′ through the open ρ ring and return on the outside. The inset shows details of RNA binding at ρ_6^{PBS}. The 5′-portion of the RNA and selected ρ_6^{PBS} residues are shown as sticks colored by atom type. Color code for this and later figures: red, carbon RNA; magenta, carbon ρ residues; light red, oxygen; blue, nitrogen; orange, phosphorus. (**C**) Quantification of β-gal activity derived from a reporter construct (scheme) in cells with ρ^{WT} or ρ^{Y80C} in the presence of the indicated plasmid-encoded β′ variants. Values represent means ± SEM of at least nine independent experiments.
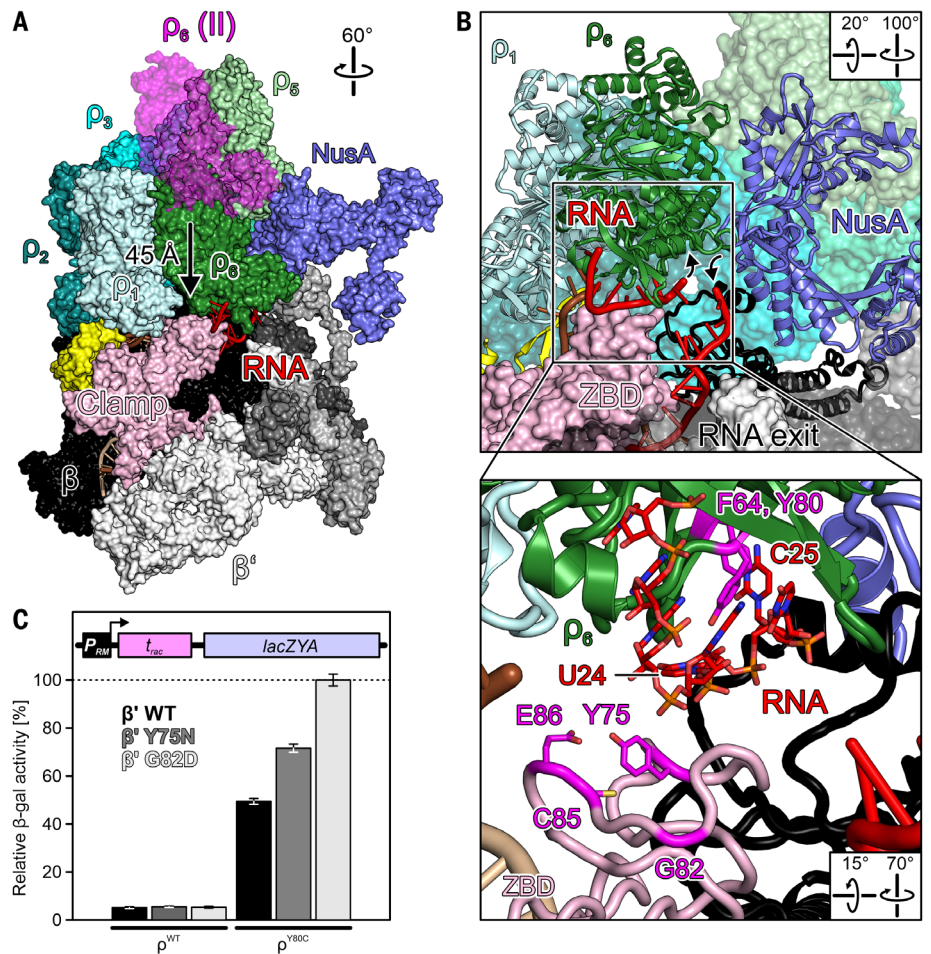
termination. To test this idea, we determined ρ effects on RNAPs lacking these elements. Whereas the lid deletion increased termination by more than a factor of 2 ($P < 0.001$), as expected, deletions of the SI3 and jaw had minor effects (Fig. 6C), in apparent contradiction to our hypothesis. However, Δjaw and ΔSI3 enzymes are pause-insensitive and are thus expected to be strongly resistant to ρ. Our results show that decreased pausing (fig. S10D) and increased susceptibility to ρ-induced allosteric changes (Fig. 6C) may cancel out, yielding near–wild-type termination. By comparison, the lid deletion does not alter elongation and its effects on ρ are direct. We stress that interpretation of these and other enzymes' sensitivities to ρ necessitates evaluation of their responses to other signals that modulate elongation.

Complex IV, with a partially open clamp, lost NusG^{NTD}, and destabilized templating nucleotide, represents a further step toward the ρ-induced RNAP inactivation. We thus termed it the inhibited complex.

EC inactivation

In complex V, RNAP is fully inactivated. The tip of the β′ clamp helices is displaced from the dDNA duplex by ~19 Å (Fig. 6D) while β′^{SI3}

and β′^{jaw} return to their positions in complex III, indicating that RNAP has lost its firm grip on dDNA. The rearrangements result in an opening of the primary channel (β$^{gate\ loop}$ Glu^{374} to β′^{clamp} Glu^{162}) from ~16 Å in complex III to ~30 Å in complex V. This opening is wide enough to allow escape of dDNA, which is further destabilized by a reorganization of β′^{rudder} and β′$^{switch\ 2}$ (which guides nucleic acids near the active site in elongation-competent ECs) and by complete collapse of the lid (Fig. 7A). However, dDNA remains in place, held back by further rearrangements: The entire RNA:DNA hybrid swings into a pseudo-continuous helix with dDNA, displacing the RNA 3′-end ~35 Å from the active site (Fig. 7B) and shifting proximal uDNA back to its position in complex III. Complex V thus represents a trapped complex postulated by Nudler and colleagues (20). Remarkably, ρ achieves RNAP inactivation while remaining in an open state.

Our findings are at odds with the kinetic coupling model (8), which explains why ρ releases RNAP at pause sites and why fast RNAPs are resistant to termination. However, fast RNAPs do not display markedly increased pause-free rates (41), which suggests that their

resistance to pausing, rather than a faster rate of RNA synthesis, confers protection against ρ. In support of this idea, we found that a pause-resistant β^{V550A} RNAP that is only marginally faster than the wild-type enzyme (46 versus 36 nucleotides/s) (41) was also resistant to ρ (31% RT RNA as compared to 15% for wild-type RNAP; $P < 0.0001$; Fig. 7C). In startling contrast, altering the rate of elongation by titrating nucleoside triphosphates (NTPs) had little effect; when NTP concentrations were increased from 25 to 200 μM, a change that enhances the rate of elongation by a factor of 6 (42), termination by wild-type RNAP was decreased by only a factor of ~1.1 (Fig. 7D). We conclude that the RNAP propensity to undergo conformational changes associated with pausing determines its sensitivity to ρ.

Discussion

Our findings suggest a pathway for ρ-mediated EC disassembly in which RNAP and the general transcription factors NusA and NusG play key roles (Fig. 8 and movie S2). We presume that ρ can passively traffic on an EC in an open configuration, because the ring closure inhibitor bicyclomycin (31) does not alter early ρ occupancy (19). At a pause site, ρ engages the
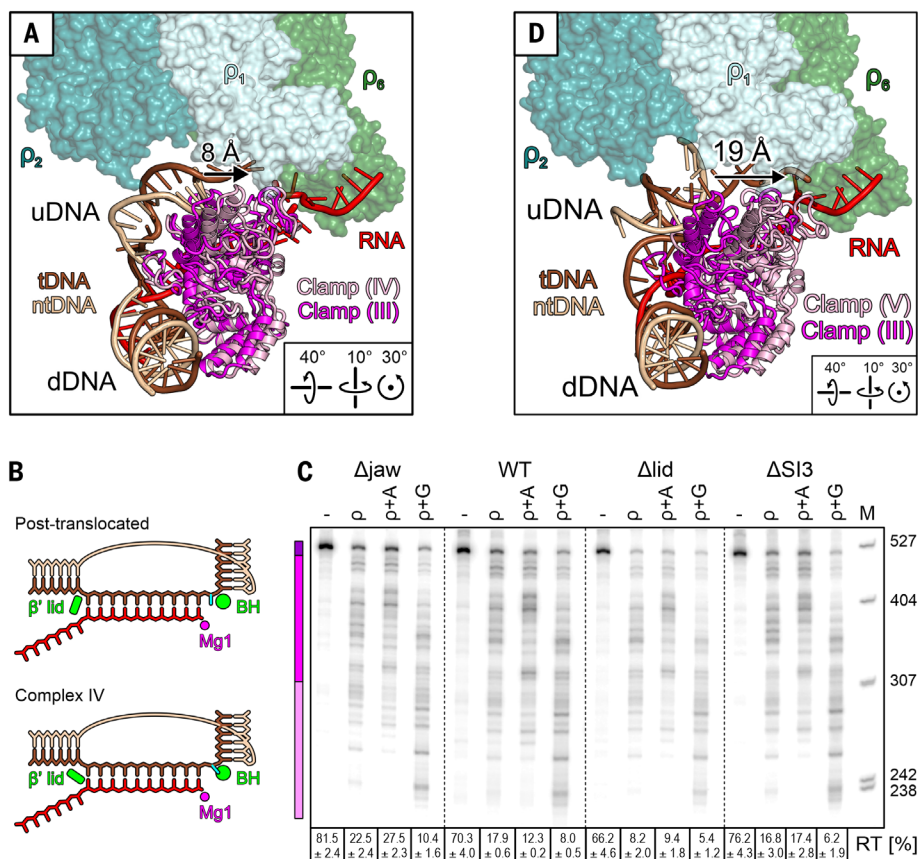
Fig. 6. Inhibition. (**A**) Comparison of selected elements of the inhibited complex (regular colors) with the β′ clamp of the RNA capture complex (magenta), illustrating partial clamp opening (arrow). (**B**) tDNA is post-translocated in complexes I to III, but the β′ lid moves and the +1 nucleotide is rotated out of the templating position in complex IV. The templating nucleotide is shown in cyan. BH, bridge helix; Mg1, catalytic magnesium ion. (**C**) Effects of deleting β′ jaw, lid, or SI3, alone or in the presence of NusA or NusG. Reactions were run on the same gel; dashed lines indicate positions where intervening lanes were removed. (**D**) Comparison of selected elements of the moribund complex (regular colors) with the β′ clamp of the RNA capture complex (magenta), illustrating clamp opening (arrow).

EC, contacting NusA, NusG[NTD], and several circularly arranged elements on RNAP, with NusA wedged between ρ_1 and ρ_6 (engagement complex). ρ_1 locally melts uDNA with the help of NusG[HL], and distal uDNA is directed toward β′[ZBD], causing NusA to rotate underneath ρ_6, preparing ρ_6 for *rut* RNA binding (primed complex). The uplifted ρ_6[PBS] captures *rut* RNA and steps down onto β′[ZBD], displacing distal uDNA (RNA capture complex); the nascent RNA that loops between ρ_6[PBS] and RNAP may be guided into the open ring. By pressing on NusG[NTD], the proximal uDNA duplex may facilitate NusG[NTD] detachment, initiating clamp opening and inhibiting tDNA translocation (inhibited complex). Upon further clamp opening, RNAP loses its grip on the nucleic acids, allowing the hybrid to dislodge from the active site (moribund complex).

Notably, we also observe structures that represent intermediates between the RNA capture and inhibited complexes (IIIa; intermediate displacement of proximal uDNA and clamp opening) (fig. S1E) and between the inhibited and moribund complexes (IVa; intermediate clamp opening and hybrid displacement) (fig. S1I), which strongly support a continuous path from complex III to complex V. However, we recognize that some of our complexes may represent different modes by which ρ directly engages a paused EC (Fig. 8, dashed arrow). We note that other configurations, representing either extra steps in a continuous pathway or additional forms of ρ attack, likely exist.

Our ρ-EC preparation contained ADP-BeF$_3$, *rut* RNA, and NusG, all of which support ring closure (*13*), yet ρ remained open throughout all stages imaged here. In fact, only the open ρ can realize all observed contacts to the EC and several ρ[PBS]s are inaccessible to RNA. Thus, the ρ-EC conformation is incompatible with ring closure, preventing immediate ter-

mination upon ρ engagement. We envision that the moribund EC is only marginally stable and will eventually allow ρ ring closure and subsequent ρ dissociation from the EC. Astonishingly, cryo-EM has allowed us to capture the transient moribund state (Fig. 7, A and B, and fig. S1J), possibly because we designed the nascent RNA to be just below the length sufficient to fill all ρ[PBS]s and added ADP-BeF$_3$ only after incubating ρ with the NusA/NusG-EC. Loss of NusG[NTD] will facilitate ρ subunits linking up with the NusA-bound end during subsequent ring closure. With RNAP wide open, upon ring closure ρ may detach with bound nucleic acids, followed by release of RNA from DNA (Fig. 8). Alternatively, ρ may translocate and release the stalled EC, either while remaining bound via a subset of contacts or after disengagement. Thus, our results do not exclude the possibility that ρ eventually closes and translocates the RNA.

Irrespective of its precise details, our model stands in stark contrast to the textbook model, in which ρ first engages the nascent RNA and uses its ATP-powered motor to translocate toward RNAP. Upon encounter, it was suggested that ρ might push RNAP forward (*43*) or pull RNA from the catalytic cleft (*44*). The latter mode of action is used by some spliceosomal RNA helicases to act from a distance (*45*). However, evidence for the direct role of translocase/helicase activity in EC dissociation by ρ is currently missing. Instead, observations that *E. coli* ρ can be replaced by phage T4 RNA:DNA helicase UvsW or RNaseH (*6*) argue that, although critical for cell viability, RNA:DNA unwinding can be uncoupled from transcription.

The textbook, RNA-dependent ρ recruitment could be used in some circumstances, but our results strongly argue against this mechanism representing the major physiological pathway of termination. Decades of in vitro experimentation have shown that after ρ loads onto a perfect *rut* site, it can strip off any obstacle from RNA. However, in the cell, ρ must terminate synthesis of all useless RNAs, whether or not they have *rut* sites (*2*), and appears to engage RNAP at the promoter (*19*). If ρ failed to bind to RNAP early on, it is certainly capable of binding to an exposed *rut* site, but this RNAP-independent targeting poses two major quandaries for ρ, which needs to (i) select RNAs that are still attached to RNAP and (ii) avoid being trapped on high-affinity RNAs. Our results show that ρ directly binds RNAP and captures RNA later, thereby selecting nascent transcripts from a vast pool of cellular RNAs.

Each step in our proposed pathway could serve as a potential checkpoint for regulation. Because ρ in each of these states realizes similar types and extents of contacts to the EC, the pathway could be readily reversible, allowing ρ to probe the RNA sequence. If no *rut* site
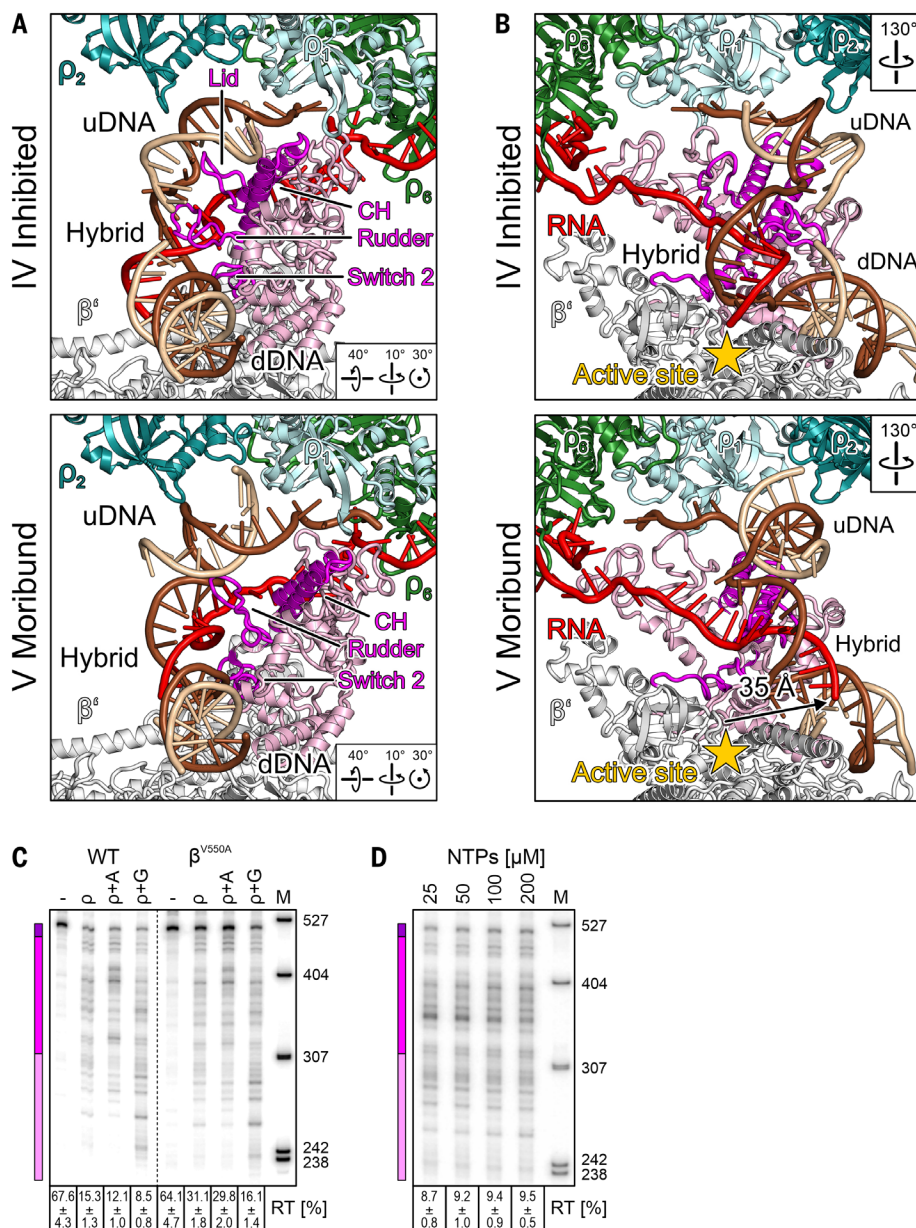
Fig. 7. Inactivation. (**A** and **B**) Side-by-side comparison of selected elements in the inhibited complex (top) and in the moribund complex (bottom), highlighting movement of the β′ clamp helices (CH, magenta) and nucleic acid–guiding loops (lid/rudder/switch 2, magenta) (A), as well as repositioning of the hybrid and displacement of the RNA 3′-end from the active site (arrow) (B). (**C**) Pause-resistant β^V550A substitution decreases ρ termination. Reactions were run on the same gel; a dashed line indicates the splice position. (**D**) Effects of NTP concentration at λ tR1.

to the primed complex lacking NusG (fig. S4). Thus, NusG^NTD may stabilize additional intermediate steps and influence the pathway reversibility. As NusA seems to initially prevent RNA capture by ρ (Fig. 1), there is a regulatory potential via a particular RNA region exhibiting differential affinities to NusA or ρ PBS. Structural comparisons reveal how transcription anti-termination complexes (23, 24) or a closely trailing ribosome (37, 38) can fend off ρ by erecting physical barriers (fig. S12).

NusG also modulates ρ-mediated termination via its CTD by promoting ring closure on suboptimal RNAs (13, 18), and mutations at the crystallographically defined NusG^CTD-ρ^CTD interface (13) lead to termination defects in vivo (34, 46); NusG^CTD sequestration by NusE (S10) in anti-termination complexes (23, 24) and a coupled ribosome (37, 38) is thought to underpin their resistance to ρ. Surprisingly, none of our refined maps revealed density for NusG^CTD. In the binary complex, NusG^CTD appears to capture and stabilize the dynamic ρ ring in a closed state (13). In our structures, the ring is held open by multiple interactions with EC components, likely inhibiting stable NusG^CTD binding. We thus can only speculate how NusG^CTD could affect the suggested pathway. It is possible that, via transient contacts not captured here, NusG^CTD (i) mediates transitions between ρ-EC states or (ii) serves to retain NusG in the complex after clamp opening (Fig. 6, A and D) and perhaps promotes subsequent ring closure.

Taken together, the available data clearly support a model in which ρ hitchhikes on RNAP and subsequently traps it in a moribund state (20). This contrasts with "torpedo" termination mechanisms (47, 48), in which exoribonucleases engage the upstream RNA after cleavage and must catch up with the EC for timely dissociation. Slowing RNAPII down upon entry into a polyadenylation site (47) promotes recruitment of cleavage factors (49) and subsequent EC capture by "torpedo" exonucleases (50). Yet ample support for a hybrid model that incorporates allosteric effects also exists (47).

All transcription termination mechanisms must trigger dissociation of a stable EC. Although the nucleic acid signals and protein factors that elicit termination differ across life, the structures of the ECs are remarkably similar, which suggests that termination signals may act upon analogous key elements, such as the clamp and the RNA:DNA hybrid. The exact sequence of events during EC dissociation remains to be determined and may differ for different termination scenarios, but there is evidence that allosteric effects contribute to termination. In bacteria, termination of most genes is triggered by formation of an RNA hairpin. Among different models of hairpin-induced termination (9), one posits

is available, the pathway may be halted prior to RNA capture. If ρ encounters a perfect *rut*, termination will ensue with a high probability, whereas a suboptimal *rut* may support termination with an intermediate likelihood. Likewise, if some of our structures represent independent attempts by ρ to terminate, rather than a continuous pathway, each state will have different probability to lead to termination. Both scenarios also provide an explanation for ρ terminating throughout a window

rather than at a specific site, as the process may be interrupted and reversed in every case, necessitating several attempts of ρ at termination.

The proposed pathway also provides insights into regulation by RNAP-associated factors. For example, our hierarchical clustering analysis showed that although the engagement and the RNA capture complexes can form in the absence of NusG (complexes I^ΔNusG and III^ΔNusG), we do not find particles conforming

Fig. 8. Model for an EC-dependent ρ-mediated termination pathway. Trafficking and termination/hybrid unwinding correspond to hypothetical steps (behind semitransparent gray boxes) preceding and following the stages resolved by cryo-EM in this work. Legend is at lower right and bottom. Coloring as in structural figures, except: DNA, upstream to downstream progressively lighter brown; hybrid, orange.

that the hairpin allosterically inactivates the EC (*51*), acting similarly to ρ in our structures. Furthermore, clamp opening for DNA release during intrinsic termination (*52*) seems to parallel the ρ-mediated mechanism detailed here. In eukaryotes, the RNA/DNA helicase Sen1, a functional analog of ρ, releases RNAPII from noncoding RNAs and must interact with RNAPII to elicit efficient termination (*53*) via a long-lived inactive EC intermediate (*54*). Thus, a sequential trap/release strategy emerges as a ubiquitous mechanism of termination.

REFERENCES AND NOTES

1. J. W. Roberts, Termination factor for RNA synthesis. *Nature* **224**, 1168–1174 (1969). doi: 10.1038/2241168a0; pmid: 4902144
2. J. M. Peters *et al.*, Rho and NusG suppress pervasive antisense transcription in Escherichia coli. *Genes Dev.* **26**, 2621–2633 (2012). doi: 10.1101/gad.196741.112; pmid: 23207917
3. C. J. Cardinale *et al.*, Termination factor Rho and its cofactors NusA and NusG silence foreign DNA in E. coli. *Science* **320**, 935–938 (2008). doi: 10.1126/science.1152763; pmid: 18487194
4. N. Sedlyarova *et al.*, sRNA-Mediated Control of Transcription Termination in E. coli. *Cell* **167**, 111–121.e13 (2016). doi: 10.1016/j.cell.2016.09.004; pmid: 27662085
5. D. Dutta, K. Shatalin, V. Epshtein, M. E. Gottesman, E. Nudler, Linking RNA polymerase backtracking to genome instability in

E. coli. *Cell* **146**, 533–543 (2011). doi: 10.1016/j.cell.2011.07.034; pmid: 21854980
6. J. K. Leela, A. H. Syeda, K. Anupama, J. Gowrishankar, Rho-dependent transcription termination is essential to prevent excessive genome-wide R-loops in Escherichia coli. *Proc. Natl. Acad. Sci. U.S.A.* **110**, 258–263 (2013). doi: 10.1073/pnas.1213123110; pmid: 23251031
7. N. D. Thomsen, M. R. Lawson, L. B. Witkowsky, S. Qu, J. M. Berger, Molecular mechanisms of substrate-controlled ring dynamics and substepping in a nucleic acid-dependent hexameric motor. *Proc. Natl. Acad. Sci. U.S.A.* **113**, E7691–E7700 (2016). doi: 10.1073/pnas.1616745113; pmid: 27856760
8. D. J. Jin, R. R. Burgess, J. P. Richardson, C. A. Gross, Termination efficiency at rho-dependent terminators depends on kinetic coupling between RNA polymerase and rho. *Proc. Natl. Acad. Sci. U.S.A.* **89**, 1453–1457 (1992). doi: 10.1073/pnas.89.4.1453; pmid: 1741399
9. J. M. Peters, A. D. Vangeloff, R. Landick, Bacterial transcription terminators: The RNA 3'-end chronicles. *J. Mol. Biol.* **412**, 793–813 (2011). doi: 10.1016/j.jmb.2011.03.036; pmid: 21439297
10. W. H. Lang, T. Platt, R. H. Reeder, Escherichia coli rho factor induces release of yeast RNA polymerase II but not polymerase I or III. *Proc. Natl. Acad. Sci. U.S.A.* **95**, 4900–4905 (1998). doi: 10.1073/pnas.95.9.4900; pmid: 9560200
11. Z. Pasman, P. H. von Hippel, Regulation of rho-dependent transcription termination by NusG is specific to the Escherichia coli elongation complex. *Biochemistry* **39**, 5573–5585 (2000). doi: 10.1021/bi992658z; pmid: 10820031
12. A. Schwartz, E. Margeat, A. R. Rahmouni, M. Boudvillain, Transcription termination factor rho can displace streptavidin from biotinylated RNA. *J. Biol. Chem.* **282**, 31469–31476 (2007). doi: 10.1074/jbc.M706935200; pmid: 17724015
13. M. R. Lawson *et al.*, Mechanism for the Regulated Control of Bacterial Transcription Termination by a Universal Adaptor Protein. *Mol. Cell* **71**, 911–922.e4 (2018). doi: 10.1016/j.molcel.2018.07.014; pmid: 30122535
14. Y. Xu, H. Kohn, W. R. Widger, Mutations in the rho transcription termination factor that affect RNA tracking. *J. Biol. Chem.* **277**, 30023–30030 (2002). doi: 10.1074/jbc.M111009200; pmid: 12034708
15. M. C. Schmidt, M. J. Chamberlin, Binding of rho factor to Escherichia coli RNA polymerase mediated by nusA protein. *J. Biol. Chem.* **259**, 15000–15002 (1984). pmid: 6096352
16. L. F. Lau, J. W. Roberts, Rho-dependent transcription termination at lambda R1 requires upstream sequences. *J. Biol. Chem.* **260**, 574–584 (1985). pmid: 2981220
17. C. M. Burns, L. V. Richardson, J. P. Richardson, Combinatorial effects of NusA and NusG on transcription elongation and Rho-dependent termination in Escherichia coli. *J. Mol. Biol.* **278**, 307–316 (1998). doi: 10.1006/jmbi.1998.1691; pmid: 9571053
18. V. Valabhoju, S. Agrawal, R. Sen, Molecular Basis of NusG-mediated Regulation of Rho-dependent Transcription Termination in Bacteria. *J. Biol. Chem.* **291**, 22386–22403 (2016). doi: 10.1074/jbc.M116.745364; pmid: 27605667
19. R. A. Mooney *et al.*, Regulator trafficking on bacterial transcription units in vivo. *Mol. Cell* **33**, 97–108 (2009). doi: 10.1016/j.molcel.2008.12.021; pmid: 19150431
20. V. Epshtein, D. Dutta, J. Wade, E. Nudler, An allosteric mechanism of Rho-dependent transcription termination. *Nature* **463**, 245–249 (2010). doi: 10.1038/nature08669; pmid: 20075920
21. J. Loerke, J. Giesebrecht, C. M. Spahn, Multiparticle cryo-EM of ribosomes. *Methods Enzymol.* **483**, 161–177 (2010). doi: 10.1016/S0076-6879(10)83008-3; pmid: 20888474
22. X. Guo *et al.*, Structural Basis for NusA Stabilized Transcriptional Pausing. *Mol. Cell* **69**, 816–827.e4 (2018). doi: 10.1016/j.molcel.2018.02.008; pmid: 29499136
23. Y. H. Huang *et al.*, Structure-Based Mechanisms of a Molecular RNA Polymerase/Chaperone Machine Required for Ribosome Biosynthesis. *Mol. Cell* **79**, 1024–1036.e5 (2020). doi: 10.1016/j.molcel.2020.08.010; pmid: 32871103
24. F. Krupp *et al.*, Structural Basis for the Action of an All-Purpose Transcription Anti-termination Factor. *Mol. Cell* **74**, 143–157.e5 (2019). doi: 10.1016/j.molcel.2019.01.016; pmid: 30795892
25. J. Y. Kang *et al.*, Structural basis of transcription arrest by coliphage HK022 Nun in an Escherichia coli RNA polymerase elongation complex. *eLife* **6**, e25478 (2017). doi: 10.7554/eLife.25478; pmid: 28318486
26. J. Y. Kang *et al.*, Structural Basis for Transcript Elongation Control by NusG Family Universal Regulators. *Cell* **173**, 1650–1662.e14 (2018). doi: 10.1016/j.cell.2018.05.017; pmid: 29887376

27. K. Schweimer et al., NusA interaction with the α subunit of E. coli RNA polymerase is via the UP element site and releases autoinhibition. *Structure* **19**, 945–954 (2011). doi: 10.1016/j.str.2011.03.024; pmid: 21742261

28. M. Z. Qayyum, D. Dey, R. Sen, Transcription Elongation Factor NusA Is a General Antagonist of Rho-dependent Termination in Escherichia coli. *J. Biol. Chem.* **291**, 8090–8108 (2016). doi: 10.1074/jbc.M115.701268; pmid: 26872975

29. J. P. Richardson, Activation of rho protein ATPase requires simultaneous interaction at two kinds of nucleic acid-binding sites. *J. Biol. Chem.* **257**, 5760–5766 (1982). pmid: 6175630

30. E. Skordalakes, J. M. Berger, Structure of the Rho transcription terminator: Mechanism of mRNA recognition and helicase loading. *Cell* **114**, 135–146 (2003). doi: 10.1016/S0092-8674(03)00512-9; pmid: 12859904

31. M. R. Lawson, K. Dyer, J. M. Berger, Ligand-induced and small-molecule control of substrate loading in a hexameric helicase. *Proc. Natl. Acad. Sci. U.S.A.* **113**, 13714–13719 (2016). doi: 10.1073/pnas.1616749113; pmid: 27821776

32. R. A. Mooney, K. Schweimer, P. Rösch, M. Gottesman, R. Landick, Two structurally independent domains of E. coli NusG create regulatory plasticity via distinct interactions with RNA polymerase and regulators. *J. Mol. Biol.* **391**, 341–358 (2009). doi: 10.1016/j.jmb.2009.05.078; pmid: 19500594

33. M. Kainz, R. L. Gourse, The C-terminal domain of the alpha subunit of Escherichia coli RNA polymerase is required for efficient rho-dependent transcription termination. *J. Mol. Biol.* **284**, 1379–1390 (1998). doi: 10.1006/jmbi.1998.2272; pmid: 9878357

34. J. Chalissery, S. Banerjee, I. Bandey, R. Sen, Transcription termination defective mutants of Rho: Role of different functions of Rho in releasing RNA from the elongation complex. *J. Mol. Biol.* **371**, 855–872 (2007). doi: 10.1016/j.jmb.2007.06.013; pmid: 17599352

35. R. Shashni, M. Z. Qayyum, V. Vishalini, D. Dey, R. Sen, Redundancy of primary RNA-binding functions of the bacterial transcription terminator Rho. *Nucleic Acids Res.* **42**, 9677–9690 (2014). doi: 10.1093/nar/gku690; pmid: 25081210

36. R. A. King, S. Banik-Maiti, D. J. Jin, R. A. Weisberg, Transcripts that increase the processivity and elongation rate of RNA polymerase. *Cell* **87**, 893–903 (1996). doi: 10.1016/S0092-8674(00)81996-0; pmid: 8945516

37. C. Wang et al., Structural basis of transcription-translation coupling. *Science* **369**, 1359–1365 (2020). doi: 10.1126/science.abb5317; pmid: 32820061

38. M. W. Webster et al., Structural basis of transcription-translation coupling and collision in bacteria. *Science* **369**, 1355–1359 (2020). doi: 10.1126/science.abb5036; pmid: 32820062

39. A. Weixlbaumer, K. Leon, R. Landick, S. A. Darst, Structural basis of transcriptional pausing in bacteria. *Cell* **152**, 431–441 (2013). doi: 10.1016/j.cell.2012.12.020; pmid: 23374340

40. F. Brueckner, P. Cramer, Structural basis of transcription inhibition by alpha-amanitin and implications for RNA polymerase II translocation. *Nat. Struct. Mol. Biol.* **15**, 811–818 (2008). doi: 10.1038/nsmb.1458; pmid: 18552824

41. A. M. Malinen et al., CBR antimicrobials alter coupling between the bridge helix and the β subunit in RNA polymerase. *Nat. Commun.* **5**, 3408 (2014). doi: 10.1038/ncomms4408; pmid: 24598909

42. V. Svetlov, G. A. Belogurov, E. Shabrova, D. G. Vassylyev, I. Artsimovitch, Allosteric control of the RNA polymerase by the elongation factor RfaH. *Nucleic Acids Res.* **35**, 5694–5705 (2007). doi: 10.1093/nar/gkm600; pmid: 17711918

43. J. S. Park, J. W. Roberts, Role of DNA bubble rewinding in enzymatic transcription termination. *Proc. Natl. Acad. Sci. U.S.A.* **103**, 4870–4875 (2006). doi: 10.1073/pnas.0600145103; pmid: 16551743

44. J. P. Richardson, Rho-dependent termination and ATPases in transcript termination. *Biochim. Biophys. Acta* **1577**, 251–260 (2002). doi: 10.1016/S0167-4781(02)00456-6; pmid: 12213656

45. D. R. Semlow, M. R. Blanco, N. G. Walter, J. P. Staley, Spliceosomal DEAH-Box ATPases Remodel Pre-mRNA to Activate Alternative Splice Sites. *Cell* **164**, 985–998 (2016). doi: 10.1016/j.cell.2016.01.025; pmid: 26919433

46. Y. Miwa, T. Horiguchi, K. Shigesada, Structural and functional dissections of transcription termination factor rho by random mutagenesis. *J. Mol. Biol.* **254**, 815–837 (1995). doi: 10.1006/jmbi.1995.0658; pmid: 7500353

47. J. D. Eaton, L. Francis, L. Davidson, S. West, A unified allosteric/torpedo mechanism for transcriptional termination on human protein-coding genes. *Genes Dev.* **34**, 132–145 (2020). doi: 10.1101/gad.332833.119; pmid: 31805520

48. M. Šiková et al., The torpedo effect in Bacillus subtilis: RNase J1 resolves stalled transcription complexes. *EMBO J.* **39**, e102500 (2020). doi: 10.15252/embj.2019102500; pmid: 31840842

49. P. K. Parua et al., A Cdk9-PP1 switch regulates the elongation-termination transition of RNA polymerase II. *Nature* **558**, 460–464 (2018). doi: 10.1038/s41586-018-0214-z; pmid: 29899453

50. M. A. Cortazar et al., Control of RNA Pol II Speed by PNUTS-PP1 and Spt5 Dephosphorylation Facilitates Termination by a "Sitting Duck Torpedo" Mechanism. *Mol. Cell* **76**, 896–908.e4 (2019). doi: 10.1016/j.molcel.2019.09.031; pmid: 31677974

51. V. Epshtein, C. J. Cardinale, A. E. Ruckenstein, S. Borukhov, E. Nudler, An allosteric path to transcription termination. *Mol. Cell* **28**, 991–1001 (2007). doi: 10.1016/j.molcel.2007.10.011; pmid: 18158897

52. M. J. Bellecourt, A. Ray-Soni, A. Harwig, R. A. Mooney, R. Landick, RNA Polymerase Clamp Movement Aids Dissociation from DNA but Is Not Required for RNA Release at Intrinsic Terminators. *J. Mol. Biol.* **431**, 696–713 (2019). doi: 10.1016/j.jmb.2019.01.003; pmid: 30630008

53. Z. Han et al., Termination of non-coding transcription in yeast relies on both an RNA Pol II CTD interaction domain and a CTD-mimicking region in Sen1. *EMBO J.* **39**, e101548 (2020). doi: 10.15252/embj.2019101548; pmid: 32107786

54. S. Wang, Z. Han, D. Libri, O. Porrua, T. R. Strick, Single-molecule characterization of extrinsic transcription termination by Sen1 helicase. *Nat. Commun.* **10**, 1545 (2019). doi: 10.1038/s41467-019-09560-9; pmid: 30948716

Science

Steps toward translocation-independent RNA polymerase inactivation by terminator ATPase ρ

Nelly Said, Tarek Hilal, Nicholas D. Sunday, Ajay Khatri, Jörg Bürger, Thorsten Mielke, Georgiy A. Belogurov, Bernhard Loll, Ranjan Sen, Irina Artsimovitch and Markus C. Wahl

How to stop RNA polymerase

Timely and tunable cessation of RNA synthesis is vital for cellular homeostasis. RNA helicases such as the archetypal termination factor r actively dismantle transcription complexes, but the transitory nature of termination makes the process hard to study structurally. Said *et al.* assembled ρ-bound transcription complexes and studied them using cryo–electron microscopy with an approach that captured a series of functional states en route to termination. They found an extensive and dynamic network of r interactions with RNA polymerase, nucleic acids, and accessory Nus factors. ρ mediates stepwise rearrangements of these contacts, transforming an actively transcribing complex into a moribund pretermination intermediate.

Science, this issue p. 44

ARTICLE TOOLS	http://science.sciencemag.org/content/371/6524/eabd1673
SUPPLEMENTARY MATERIALS	http://science.sciencemag.org/content/suppl/2020/11/24/science.abd1673.DC1
REFERENCES	This article cites 82 articles, 26 of which you can access for free http://science.sciencemag.org/content/371/6524/eabd1673#BIBL
PERMISSIONS	http://www.sciencemag.org/help/reprints-and-permissions

Use of this article is subject to the Terms of Service